

Highlights

A Comparative Study on Frequency-Constrained Unit Commitment Approaches in Island Power Systems

Miad Sarvarizadeh, Mohammad Rajabdorri, Enrique Lobato, Lukas Sigrist

- A comparison framework is provided to compare four frequency-constrained unit commitment methods with a base case unit commitment formulation, regarding the system benefits and computational burden perspectives.
- Two performance indices are introduced to help analyze and compare the formulations more effectively by considering the under-frequency load shedding reduction.
- Each formulation is implemented on a real Spanish island power system illustrating its effectiveness in real-world systems and helping operators choose the suitable method in different circumstances.

A Comparative Study on Frequency-Constrained Unit Commitment Approaches in Island Power Systems

Miad Sarvarizadeh^a, Mohammad Rajabdorri^a, Enrique Lobato^a, Lukas Sigrist^a

^a*IIT, Comillas Pontifical University, Madrid, Spain*

Abstract

The increasing penetration of renewable energy sources reduces rotating inertia and even frequency control capacity, affecting frequency stability. This challenge is significant in island power systems (IPS) that already suffer from low inertia and frequency control capacity. This paper presents a comparative study on different frequency-constrained unit commitment (FCUC) formulations applied to IPS. Then, by considering under-frequency load shedding as a significant measure of frequency stability in IPS, two indices are presented to fully compare the formulations from system benefits and computational burden perspectives. Simulations conducted on a real Spanish island show that the data-driven corrective FCUC formulation has the most advantages among other formulations.

Keywords: frequency-constrained unit commitment, analytical model, data-driven model, island power systems, machine learning, under frequency load shedding, computational burden

1. Introduction

1.1. Motivation

The unit commitment (UC) problem involves determining the most economically efficient scheduling of generation units in a power system. The goal of the UC problem is to minimize total system operation costs while considering system operation constraints, and all technological limitations of generation units. However, traditional UC formulations tend to ignore frequency-related constraints. Frequency stability can be added to the UC

problem leading to frequency-constrained unit commitment (FCUC) formulations.

The small size of island power systems (IPS) indicates that fewer generating units are available, resulting in lower inertia and frequency control capacity. Furthermore, the spinning reserve requirements are more demanding concerning the size of the units, leading to higher overall operation costs. Increasing the use of renewable energy sources (RES) in IPS could lower operational costs and improve sustainability. However, with more RES the already limited inertia of the system will be lower, and the frequency response following a generator outage will have less favorable characteristics [1]. Consequently, preventing under-frequency load shedding (UFLS) entirely by setting conservative frequency nadir thresholds would not be feasible in small IPS. Therefore, UFLS is inevitable for large outages in IPS [2].

Including frequency-related constraints into the UC problem of IPS causes changes from two different perspectives. From the operational perspective, the operation costs will be higher as a trade-off for better post-contingency frequency performance, improving frequency stability. The second perspective is the computational burden. Frequency constraints often add a lot of new variables and constraints to the problem and could result in higher solution times compared to the traditional UC formulations.

Different indices have been considered to evaluate the performance of an FCUC formulation for IPS. The amount of UFLS is a significant measure of frequency stability since the UFLS scheme acts when frequency stability is put at risk, i.e., when frequency deviations or rate of change of frequency (RoCoF) exceed certain thresholds by the system operator. Accordingly, the ultimate goal of the FCUC formulations in IPS is to minimize the total possible amount of UFLS after outages while imposing minimum extra costs and computational burden on the problem. This concept is the foundation of the comparison framework presented in this paper.

1.2. Literature review

To ensure power grid frequency stability following disturbances, three primary frequency indicators (RoCoF, frequency nadir, and quasi-steady-state frequency) are constrained to thresholds [3]. Adding these constraints limits the characteristics of the post-contingency frequency performance, thus forming preventive frequency-constrained unit commitment (P-FCUC) formulations. The frequency-related constraints are modeled utilizing analytical or data-driven methods.

Several papers have presented analytical P-FCUC formulations. Bernstein polynomials are used in [4] to approximate the differential-algebraic equations describing the power system. Before being implemented in the UC, the differential equations are first transformed into a set of linear equations. The dynamic response solution offers suitable restrictions by utilizing the characteristics of Bernstein polynomials. [5] presents a location-based UC formulation that is RoCoF-constrained and focuses on location-based frequency characteristic differentiation. Furthermore, the cost-benefit impact of virtual inertia is investigated. Analytical constraints for RoCoF and frequency nadir are derived in [6] based on the center of inertia concept. Moreover, random sampling of generation unit combinations is utilized to obtain lower bounds for the frequency constraints. An analytical method for modeling frequency stability constraints that includes the frequency response from RES is presented in [7]. The suggested mixed-integer non-linear programming (MINLP) problem is solved using decomposition techniques. In [8], a separable programming technique is used to model the nonlinear frequency nadir constraint in the UC problem. The frequency nadir constraint is approximated using a piece-wise linear function.

Some studies have utilized data-driven approaches to formulate P-FCUC problems. [9] presents a frequency nadir constraint using linear regression. Requirements for minimum inertia or frequency nadir are included in this model. To validate the presented model the Maui Island system is used. An extreme learning machine model is presented in [10] to obtain a linearized frequency nadir constraint. Furthermore, in the day-ahead UC problem, the droop gains and reserves of available generators are optimized to consider the variations in frequency insecurity. A deep neural network-based data-driven framework for predicting frequency nadir is described in [11] and incorporated into mixed-integer linear programming (MILP) formulations. To avoid UFLS, a region-of-interest active sampling is used to choose samples with frequency nadirs near the threshold. In [12], a sparse neural network technique based on a conservative sparse neural network is presented for approximating step-wise constraints and frequency nadir. An MILP representation of these constraints is obtained to add them to the UC problem. A data-driven approach in modeling non-linear frequency nadir constraint in the UC problem using logistic regression and support vector machine is presented in [13]. The results are provided for a real IPS and compared with an analytical method.

Corrective measures such as UFLS are utilized in power systems as a last resort to alter frequency decay [14]. A UFLS scheme automatically sheds

load based on system measurements. According to [15], these automatic UFLS schemes can be categorized as conventional or advanced. Plenty of studies have focused on designing UFLS schemes. However, few papers have studied UFLS as a corrective measure in a FCUC formulation.

Authors in [16] examined the optimal UFLS schemes to reduce the amount of shed load using predetermined generating commitment states. Similarly, [17] explores the optimal commitment of interruptible loads to ensure adequate primary frequency response, but does not consider the commitment of generating units. One of the initial studies on incorporating UFLS in the FCUC formulations is proposed in [18]. An analytical estimation of UFLS is calculated considering linear reserve provision of the units in response to a known outage. UFLS is divided into blocks, with one nadir constraint per block. Then binary variables are utilized to determine the optimal UFLS level for scheduling. A framework to co-optimize UFLS and fast and slow frequency responses is provided in [19]. The resulting non-convex estimation of UFLS is approximated with a second-order cone, which is fairly accurate. In [20] an analytical method to include UFLS that gives a corrective frequency-constrained unit commitment (C-FCUC) formulation is presented. Similarly, it is assumed that the units provide reserve linearly and the amount of power outage is known.

Estimating and co-optimizing UFLS using data-driven approaches is proposed in [21]. A learning process to estimate the amount of UFLS is presented, considering conventional schemes due to their extensive utilization. This formulation also considers the maximum RoCoF constraint, so it can be viewed as a hybrid formulation that proposes both corrective and preventive measures. This formulation is studied on a real-world Spanish IPS demonstrating its effectiveness in estimating real amounts of UFLS.

As indicated, many studies have provided FCUC formulations and successfully improved the post-contingency frequency performance of IPS. These studies can be categorized into analytical or data-driven, preventive or corrective FCUC. However, most of these studies are isolated studies that ignore comparisons to other methods and overlook the computational burden they impose on current formulations. This study tries to address the practical limitations of FCUC formulations by comparing four different methods (one for each category) from two different perspectives: system benefits and computational burden.

Figure 1 illustrates a timeline of the reviewed literature. This figure highlights the methods used in each study and shows whether they are applied

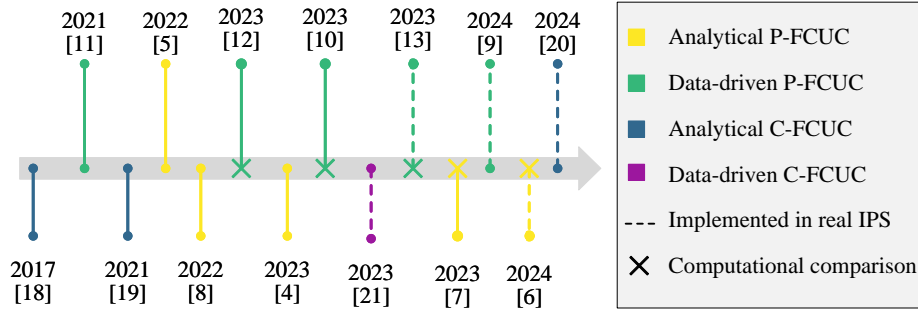


Figure 1: Timeline of the reviewed literature

to real-world IPS. Additionally, Figure 1 shows if any analysis regarding the computational burden of the formulation is presented in each paper. It is important to note that most studies that provide analysis of the computational burden, fall short of analyzing it according to the benefits they provide to the system and compare them to other methods possible.

This paper provides a framework to compare four different FCUC methods implemented in small IPS, with a base case unit commitment (BUC) formulation. Comparing FCUC methods is crucial because each one employs different simplifying assumptions and varies in computational complexity. It is essential to evaluate how accurately these methods approximate more detailed dynamic simulations, which can provide a more realistic representation of system behavior. The method in [8] is used as a representative of analytical P-FCUC, whereas the one in [13] serves as a representative of data-driven P-FCUC. An analytical C-FCUC formulation is represented by [20]. We adopted the methodology from [21], which estimates the amount of UFLS using regression trees, and integrated it into the UC problem. This implementation serves as a data-driven C-FCUC in our comparison. The code used for solving all of these formulations is available on <https://github.com/Miadsrv/FrequencyConstrainedUC>. It is important to note that although these formulations do not represent every possible formulation of FCUC, they are the main ones that are proposed for IPS considering the unique characteristics of these systems. Therefore, this study provides clear insights into the scheduling problem in IPS, considering frequency stability.

1.3. Contributions and structure

The main contributions of this paper are the following:

- A comparison framework is provided to compare four different FCUC methods with a base case UC formulation for IPS, regarding the system benefits and computational burden perspectives.
- The methodology in [21] estimates the amount of UFLS triggered by real-world schemes. Here, the estimation is incorporated into the UC problem, forming a C-FCUC model.
- Two performance indices are introduced to help analyze and compare the formulations more effectively from the system benefits and computational burden viewpoints by considering the amount of UFLS reduction.
- Each formulation is implemented on a real Spanish IPS illustrating its effectiveness in real-world IPS to help operators choose the suitable method in different circumstances.

The remainder of this paper is organized as follows: first of all, the mathematical formulation of base case UC problem and four different FCUC methods are provided in Section 2. Section 3 describes the comparison framework and the key performance indicators (KPIs). Then, Section 4 provides the obtained results. Finally, Section 5 gives some conclusions.

2. Mathematical formulation of models

The UC problem is formulated to minimize the operation cost of generators and considers various constraints. This section presents the complete formulation of BUC as the benchmark formulation. Then, the four selected FCUC formulations are presented, each representing a different category of formulations.

2.1. Base case formulation

The BUC model is a typical representation of the UC problem that includes eqs. (1a) to (1k). The objective function presented in eq. (1a) minimizes the total operation cost of the system including generation and start-up costs.

$$\begin{aligned}
\min_{u,p} c^g(p) + c^{\text{suc}}(u) & \quad (1a) \\
u_{i,t} - u_{i,t-1} = v_{i,t} - w_{i,t} & \quad \forall i, \forall t \quad (1b) \\
v_{i,t} + w_{i,t} \leq 1 & \quad \forall i, \forall t \quad (1c) \\
\sum_{s=t-\text{UT}_i+1}^t v_{i,s} \leq u_{i,t} & \quad t \in \{\text{UT}_i, \dots, \mathcal{T}\} \quad (1d) \\
\sum_{s=t-\text{DT}_i+1}^t w_{i,s} \leq 1 - u_{i,t} & \quad t \in \{\text{DT}_i, \dots, \mathcal{T}\} \quad (1e) \\
p_{i,t} \geq P_i^{\text{min}} u_{i,t} & \quad \forall i, \forall t \quad (1f) \\
p_{i,t} + r_{i,t} \leq P_i^{\text{max}} u_{i,t} & \quad \forall i, \forall t \quad (1g) \\
p_{i,t} - p_{i,t-1} \leq R_i^{\text{up}} & \quad \forall i, \forall t \quad (1h) \\
p_{i,t-1} - p_{i,t} \leq R_i^{\text{down}} & \quad \forall i, \forall t \quad (1i) \\
\left(\sum_i p_{i,t} \right) + g_t^w + g_t^s = \mathcal{D}_t & \quad \forall t \quad (1j) \\
\sum_{i \neq \ell} r_{i,t} \geq p_{\ell,t} & \quad \forall t, \ell \quad (1k)
\end{aligned}$$

Equations (1b) and (1c) represent the binary logic of the UC problem. The minimum up-time and down-time constraints are presented in eqs. (1d) and (1e). Each generator's output and reserve are constrained by the minimum and maximum capacity and ramp rate bounds through eqs. (1f) to (1i). Equation (1j) is the power balance constraint. The reserve constraint is presented in eq. (1k) that makes sure there is enough reserve to compensate for the active power disturbance of generating unit ℓ .

2.2. Preventive FCUC formulations

The dynamics of the generator rotor in power systems are usually described by the swing equation of eq. (2).

$$\frac{2H}{f_0} \frac{d\Delta f(t)}{dt} + DD_t \Delta f(t) = P_m - P_e \quad (2)$$

Formulations of P-FCUC aim to incorporate the system dynamics by analyzing the eq. (2) equation and reflecting these dynamics within the UC

problem. The objective of these formulations is to schedule generation to mitigate the risk of poor frequency responses following $N - 1$ contingencies, thereby enhancing system reliability. Preventive FCUC formulations incorporate constraints to ensure that key measures (RoCoF, quasi-steady-state frequency, and frequency nadir) remain within acceptable limits.

The maximum RoCoF constraint is presented in eq. (3) indicates the minimum level of inertia requirement based on a maximum RoCoF allowed. This linear constraint can be added directly to the BUC formulations.

$$H_\ell \geq \frac{p_\ell f_0}{2\Delta f_{\text{crit}}} \quad \forall t, \ell \quad (3)$$

For the quasi-steady-state frequency following an outage, it is assumed that it has stabilized without the secondary frequency control activation. To ensure that the quasi-steady-state frequency remains within acceptable limits, eq. (4) can be derived from the swing equation. This equation is also linear and is added directly to the formulations.

$$\sum_{i \neq \ell} r_{i,t} \geq P_\ell - DD_t \Delta f_{\text{crit}}^{\text{ss}} \quad \forall t, \ell \quad (4)$$

The frequency nadir constraint is more complicated to add to the UC problem. Analytical and data-driven methods are the two main approaches to modeling the frequency nadir which are discussed in the following.

2.2.1. Analytical nadir constraints

The analytical model of frequency nadir discussed here is based on [8] where separable programming is utilized. A key assumption in this method, widely used in the literature, is that each unit's reserve increases linearly and achieves its peak output within T seconds as indicated in eq. (5). The frequency nadir is assumed to happen before T .

$$r_{i,t}(\tau) = \begin{cases} \frac{r_{i,t}\tau}{T} & \text{if } \tau \leq T \\ r_{i,t} & \text{if } \tau > T \end{cases} \quad (5)$$

The resulting non-convex frequency nadir constraint is presented in eq. (6). Change of variables and separable programming are utilized to linearize this constraint.

$$H_\ell R_\ell - \frac{f_0 T p_\ell^2}{4\Delta f_{\text{crit}}^{\text{nadir}}} + \frac{DD_t T p_\ell f_0}{4} \geq 0 \quad \forall t, \ell \quad (6)$$

The product $H_\ell R_\ell$ is rewritten using the following variable change.

$$H_\ell \alpha R_\ell \beta = x_1^2 - x_2^2 \quad (7a)$$

$$\frac{x_1 + x_2}{\alpha} = H_\ell \quad (7b)$$

$$\frac{x_1 - x_2}{\beta} = R_\ell \quad (7c)$$

Then, by substituting eq. (7a) ineq. (6), the resulting frequency nadir equation can be written as the following:

$$\frac{x_1^2 - x_2^2}{\alpha\beta} - \frac{f_0 T p_\ell^2}{4\Delta f_{\text{crit}}^{\text{nadir}}} + \frac{DD_t T p_\ell f_0}{4} \geq 0 \quad \forall t, \ell \quad (8)$$

The remaining non-linear terms are p_ℓ^2 , x_1^2 , and x_2^2 , which can be linearized quite straightforwardly. The linearization process of these terms is presented in detail in [22].

2.2.2. Data-driven nadir constraints

Another approach to include frequency nadir constraint into the UC problem is based on the data-driven estimation of the frequency nadir by using machine learning techniques. The data-driven method discussed here is described in detail in [13]. This approach includes several steps including data generation, labeling the data set with the corresponding nadir frequency, and training the machine learning model. Here a summary of the process is presented.

A well-structured dataset of features and labels is essential to predict the frequency nadir in UC problems. The features represent operating points and are paired with labels representing the frequency nadir measurements after all possible outages. These labels are derived using dynamic system frequency response (SFR) models. Labels can be numeric (e.g. frequency in Hz) or categorical (e.g. tolerable or not).

The selected features must efficiently predict the label without overcomplicating the model. Only the most relevant features accessible in the UC problem must be chosen. The selected features for predicting frequency nadir adequacy are the sum of available inertia (H_ℓ), the weighted gain of the turbine-governor model ($\hat{K}_{\ell,t}^s$) defined in eq. (9), lost power (p_ℓ), and the sum of available reserve (R_ℓ) after the outage of generator ℓ . Then the SFR model is used to label the data set with the corresponding frequency nadir of

each possible outage. The SFR model utilizes a second-order approximation to represent the turbine-governor system of each generating unit. Details of the SFR model can be found in [1]. Note that any other power system model can be used instead of the SFR model.

$$\hat{K}_{\ell,t}^s = \sum_{i \neq \ell} \frac{K_i}{T_i} u_{i,t} \quad (9)$$

Here, a logistic regression model is utilized. The labels classify data points, where +1 represents acceptable outcomes, which means that the frequency nadir is in the acceptable range. Alternatively, 0 represents the incidents for which their corresponding frequency nadir is unacceptable. The machine learning model aims to learn a decision function $f_{\theta}(x)$ presented in eq. (10), which produces positive values for acceptable points and negative values for unacceptable ones while minimizing misclassifications.

$$f_{\theta}(x) = \theta_0 + \sum_{j=1}^J \theta_j x_j \quad (10)$$

The selected features are replaced in eq. (10), and eq. (11) is obtained.

$$\theta_0 + \theta_1 H_{\ell} + \theta_2 \hat{K}_{\ell,t}^s + \theta_3 p_{\ell} + \theta_4 R_{\ell} \geq 0 \quad (11)$$

After calculating the parameters of the eq. (11), the learned decision function can be directly added to the MILP formulation as a constraint.

2.3. Corrective FCUC formulations

The formulations covered up to this point are based on preventive measures ensuring the frequency remains within acceptable limits without taking corrective action. Depending on the system, the P-FCUC formulations might successfully prevent UFLS from happening according to the imposed critical frequency limits. This is achievable for sufficiently large systems but may lead to increased system operation costs in glsips. In addition, for small IPS, UFLS occurrences are inevitable. The smaller size implies that fewer generating units are connected, indicating that the inertia of the system and the overall frequency control capacity are lower.

Given these considerations, modeling UFLS inside the UC problem is an effective approach that enables the utilization of inevitable UFLS occurrences along with spinning reserves. This would likely reduce operation costs

as shown in Section 4 considering that a lower reserve could be scheduled. Also, the cost associated with activating UFLS can be minimized alongside the other operation costs in the objective function. Similar to the previous section, UFLS can be modeled and added to the UC problem using analytical and data-driven approaches forming a C-FCUC formulation.

2.3.1. Analytical UFLS constraints

This formulation is based on [20], estimating the amount of UFLS achievable by advanced UFLS schemes. First, the amount of generation loss that can lead to a frequency nadir that exceeds the preset acceptable threshold is presented as $p_{\ell,t}^{\text{crit}}$.

$$2H_{\ell,t}\hat{K}_{\ell,t}^s(\Delta F^{\text{nadir}})^2(S^{\text{base}})^2 = (p_{\ell,t}^{\text{crit}})^2 \quad (12)$$

In eq. (12) $H_{\ell,t}$ is the sum of available inertia after the outage of unit ℓ , ΔF^{nadir} is the frequency nadir threshold, and $\hat{K}_{\ell,t}^s$ is defined in eq. (9). Equation (12) contains two nonlinear terms. $(p_{\ell,t}^{\text{crit}})^2$ can be linearized similar to the process presented in [22]. Additionally, to linearize the binary to binary products resulting from $H_{\ell,t}\hat{K}_{\ell,t}^s$ term, first, it can be written as eq. (13).

$$H_{t,\ell}^s \times \hat{K}_{t,\ell}^s = \begin{bmatrix} \frac{K_1}{T_1} \\ \vdots \\ \frac{K_\ell}{T_\ell} \\ \vdots \\ \frac{K_n}{T_n} \end{bmatrix}^{-1} \begin{bmatrix} u_1u_1 & u_1u_2 & \dots & u_1u_\ell & \dots & u_1u_n \\ \vdots & \vdots & \vdots & \vdots & \vdots & \vdots \\ u_\ell u_1 & u_\ell u_2 & \dots & u_\ell u_\ell & \dots & u_\ell u_n \\ \vdots & \vdots & \vdots & \vdots & \vdots & \vdots \\ u_n u_1 & u_n u_2 & \dots & u_n u_\ell & \dots & u_n u_n \end{bmatrix} \begin{bmatrix} H_1 \\ \vdots \\ H_\ell \\ \vdots \\ H_n \end{bmatrix} \quad (13)$$

The matrix containing binary-to-binary products is symmetric and the diagonal elements like u_iu_i do not need to be linearized. The rest are linearized using the constraints presented in [20].

If the outage is larger than $p_{\ell,t}^{\text{crit}}$, UFLS will be activated. Alternatively, if the outage is smaller than $p_{\ell,t}^{\text{crit}}$, no UFLS will be activated. The amount of UFLS is calculated in eq. (14). This value of UFLS can be used as an estimation inside the UC problem.

$$p_{\ell,t}^{\text{UFLS}} = \begin{cases} p_{\ell,t} - p_{\ell,t}^{\text{crit}} & \text{if } p_{\ell,t} > p_{\ell,t}^{\text{crit}} \\ 0 & \text{otherwise.} \end{cases} \quad (14)$$

Equation (14) is linearized here using the method presented in [23]. The following set of constraints substitute eq. (14).

$$p_{\ell,t} - p_{\ell,t}^{\text{crit}} = p_{\ell,t}^{\text{UFLS}} - e_{\ell,t} \quad (15a)$$

$$p_{\ell,t}^{\text{UFLS}} \leq M u'_{\ell,t} \quad (15b)$$

$$e_{\ell,t} \leq M(1 - u'_{\ell,t}) \quad (15c)$$

In eq. (15), $e_{\ell,t}$ is an auxiliary variable, $u'_{\ell,t}$ is a binary activation variable, and M is a sufficiently large number. This set of constraints ensure that either $p_{\ell,t}^{\text{UFLS}}$ or $e_{\ell,t}$ is zero. This can alternatively be done using the indicator constraints that modern solvers widely accept.

Then, another constraint is applied to guarantee that each generating unit can deliver the reserve on time. Equation (16) accounts for the distribution of the available reserve. It ensures that the remaining units after the outage will have enough headroom, relative to their speed of response.

$$p_{i,t} + \frac{\hat{K}_i u_{i,t}}{\hat{K}_{\ell,t}^s} p_{\ell,t}^{\text{crit}} \leq P_i^{\text{max}} u_{i,t} \quad \forall t, \ell \quad (16)$$

Equation (16) contains several non-linear terms. The primary focus is on enforcing eq. (16) for online units. In this case, we assume that $u_{i,t}$ is equal to one and introduce an additional term to consistently satisfy the constraint for offline units (where $u_{i,t}$ equals zero). Accordingly, eq. (16) is updated as follows:

$$p_{i,t} \hat{K}_{\ell,t}^s + \hat{K}_i p_{\ell,t}^c \leq P_i^{\text{max}} \hat{K}_{\ell,t}^s + M(1 - u_{i,t}) \quad \forall i \neq \ell \quad (17)$$

Here, M represents a sufficiently large number, leaving the only remaining non-linear term $p_{i,t} \hat{K}_{\ell,t}^s$. Each resulting non-linear term is a binary in a continuous variable product as indicated before it can be passed to the solver as indicator constraints or linearized by the big- M method presented in [20].

The final step is to modify the objective function and the reserve constraint of UC to co-optimize UFLS alongside operation costs. Equation (18) presents the modified objective function used here.

$$\min_{u,p} c^g(p) + c^{\text{suc}}(u) + c^{\text{UFLS}}(p^{\text{UFLS}}) \quad (18)$$

where,

$$c^{\text{UFLS}}(p^{\text{UFLS}}) = \sum_t \sum_i c_{\text{UFLS}}^o \times \text{FOR}_i \times p_{i,t}^{\text{UFLS}} \quad (19)$$

Here, c_{UFLS}^o is the post-outage cost of UFLS in €/MW and FOR is the forced outage rate of generators in %.

Moreover, since an estimation of the UFLS that will happen after each outage is available now in the optimization problem, the reserve constraint should be modified to schedule less reserve according to the estimation of UFLS. The reserve constraint used in this formulation is presented in eq. (20).

$$\sum_{i \neq \ell} r_{i,t} \geq p_{\ell,t} - p_{\ell,t}^{\text{UFLS}} \quad \forall t, \ell \quad (20)$$

2.3.2. Data-driven UFLS constraints

An alternative approach to modeling UFLS inside the UC problem and forming a C-FCUC formulation is data-driven estimation of UFLS using machine learning techniques. The method implemented in this section is based on [21]. This method uses the same data set as in Section 2.2.2. The same set of features are selected to represent the data points. However, this time the data points are labeled with the corresponding amount of UFLS using the SFR model. This model can calculate the amount of UFLS based on the traditional UFLS schemes used predominately in power systems. This allows the integration of real UFLS schemes into the problem and a more realistic estimation of UFLS compared to the analytical formulation.

Using the labeled data set, a regression tree structure is utilized here to estimate the amount of UFLS. The regression tree employs logistic regression and gives a linear function of features to classify the UFLS predictions into three different categories. Then, within each resulting leaf, linear regression is used to estimate the values of UFLS. The tree structure must be as simple as possible, to enable efficient integration into an MILP formulation.

To model the UFLS estimation inside the UC problem, the tree structure must be represented as MILP equations. A binary variable is assigned to each leaf allowing activation of one leaf to estimate UFLS. Equation (21) enforces only one of these binary variables to equal 1.

$$\sum_{\ell e \in \mathcal{L}} z_{\ell e} = 1 \quad (21)$$

Then the resulting logistic regression linear functions of features after training the model, are used to represent classifications in MILP form. Equation (22) shows the set of constraints utilized for the classification in the first

node. Another set of similar constraints must be added for the second classification.

$$\hat{\beta}_0 + \sum_{j=1}^J \hat{\beta}_j x_j + \underline{M} \sum_{\ell e \in \mathcal{L}'} z_{\ell e} \geq \underline{M} \quad (22a)$$

$$\hat{\beta}_0 + \sum_{j=1}^J \hat{\beta}_j x_j + \overline{M} \sum_{\ell e \in \mathcal{L}''} z_{\ell e} < \overline{M} \quad (22b)$$

Where, $\hat{\beta}$ are the logistic regression coefficients, and \underline{M} and \overline{M} are big negative and positive numbers respectively. \mathcal{L}' and \mathcal{L}'' are the list of leaves in the right and left subtrees of the node N_0 .

When the classification is performed, linear regression is used in any chosen leaf to estimate UFLS. The following constraint calculates UFLS using linear regression functions.

$$p^{\text{UFLS}} = \sum_{\ell e \in \mathcal{L}} z_{\ell e} \times \left(\alpha_0^{\ell e} + \sum_{j=1}^J \alpha_j^{\ell e} x_j \right) \quad (23)$$

Where α_j are the linear regression coefficients. Equation (23) must be linearized using the indicator constraint option of the MILP solvers or the big- M method so that it can be added to the MILP formulation [20].

Like the previous formulation, the objective function and the reserve constraint must be changed. The objective function is changed to eq. (18) to co-optimize UFLS alongside operation costs. The resulting reserve constraint used in this formulation is presented in eq. (24).

$$r_{i,t} \geq \frac{\hat{K}_i u_{i,t}}{\hat{K}_{\ell,t}^s} (p_{\ell,t} - p_{\ell,t}^{\text{UFLS}}) \quad \forall t, \ell \quad (24)$$

Analogous to the eq. (16), eq. (24) is simplified and then linearized [20].

2.4. Definition of models

To clearly distinguish the different models discussed in the previous subsections, each model is clearly defined with the corresponding constraints in Table 1. The maximum RoCoF constraint presented in eq. (3) is added to the analytical C-FCUC formulation to achieve a more fair comparison. It is important to note that the non-linear constraints should be linearized before being added to the formulation, as discussed earlier.

Table 1: Model definitions

| model | mutual constraints | unique constraints |
|--------------------|--------------------|---------------------------------------|
| BUC | | eqs. (1a) and (1k) |
| analytical P-FCUC | | eqs. (1a), (3), (4), (7) and (8) |
| data-driven P-FCUC | eqs. (1b) to (1j) | eqs. (1a), (3), (4), (9) and (11) |
| analytical C-FCUC | | eqs. (3), (12), (14) and (18) to (20) |
| data-driven C-FCUC | | eqs. (3), (18) and (21) to (24) |

3. Comparison framework

Two perspectives are evaluated to compare different FCUC thoroughly formulations. First, the system benefits are analyzed in terms of the operation cost, and the total UFLS for all possible outages. The operation cost and total UFLS are the main KPIs that help compare the effectiveness of the formulations in real operation conditions of island power systems. The amount of UFLS is calculated using the SFR model. The SFR model captures the short-term frequency response of a power system using a second-order model approximation to represent the turbine-governor system of the generating units. The excitation and generator transients are neglected due to their faster response times. The detailed model is presented in [1].

The second perspective analyzed here is the computational burden imposed by each formulation. To compare the computational burden of each model, metrics like the CPU time each formulation takes to reach a solution using a relative optimality tolerance of 0.1%, and the compactness of each formulation in terms of the number of total variables, discrete variables, and constraints are presented.

Additionally, the sensitivity of each model to its relevant threshold is analyzed. The preventive formulations are simulated using different nadir thresholds, and the corrective formulations are simulated with different UFLS costs. This would show how these formulations can adapt to the level of operation security in various situations.

Table 2: Parameters of the Generating Units

| unit | P^{\max} (MW) | P^{\min} (MW) | M^{base} (MVA) | H (s) | K (pu) |
|-------------|--------------------|--------------------|----------------------------|---------|----------|
| 1 | 3.82 | 2.35 | 5.4 | 1.75 | 20 |
| 2 | 3.82 | 2.35 | 5.4 | 1.75 | 20 |
| 3 | 3.82 | 2.35 | 5.4 | 1.75 | 20 |
| 4 | 4.3 | 2.82 | 6.3 | 1.73 | 20 |
| 5 | 6.7 | 3.3 | 9.4 | 2.16 | 20 |
| 6 | 6.7 | 3.3 | 9.6 | 1.88 | 20 |
| 7 | 11.2 | 6.63 | 15.75 | 2.1 | 20 |
| 8 | 11.5 | 6.63 | 14.5 | 2.1 | 20 |
| 9 | 11.5 | 6.63 | 14.5 | 2.1 | 20 |
| 10 | 11.5 | 6.63 | 14.5 | 2.1 | 20 |
| 11 | 21 | 4.85 | 26.82 | 6.5 | 21.25 |

4. Results

4.1. Case study description

All the mentioned formulations are tested using data from a sample day in the power system of a real Spanish island. The generation mix includes eleven diesel generators and about 10% of its annual demand is provided by wind and solar power generation. Additionally, the real UFLS settings of the system are used to calculate UFLS in the SFR model so that a realistic comparison of the resulting UFLS amounts can be performed. Parameters of the diesel generators are provided in Table 2.

The formulations are all simulated in GAMS, and Gurobi 10.0.3 is used as the solver with default settings. The simulations were run on an Intel-i7-8700 CPU @ 3.20GHz with twelve threads and 32 GB of RAM. The code and sample outputs are available on <https://github.com/Miadsrv/FrequencyConstrainedUC>.

4.2. System benefits results

The simulation results of all the formulations are provided in Table 3. The operation cost of every formulation is given in k€ and the increase/decrease compared to the base case is reported in percentage. Then, the possible generator outages are simulated with the SFR dynamic simulator using the

Table 3: System benefits results

| case study | $\Delta f_{\text{crit}}^{\text{nadir}}$ (Hz) | c_{UFLS}^o (k€/MW) | operation cost (k€) | $\sum P_{\text{SFR}}^{\text{UFLS}}$ (MW) | c^{UFLS} (k€) | average nadir (Hz) |
|--------------------|--|-----------------------------|---------------------|--|------------------------|--------------------|
| base case UC | - | - | 68.15 | 358.25 | - | -1.350 |
| analytical P-FCUC | 3 | - | 71.32 (+4.7%) | 183.44 (-48.8%) | - | -1.150 |
| | 2.8 | - | 71.39 (+4.8%) | 189.63 (-47.1%) | - | -1.156 |
| | 2.6 | - | 71.46 (+4.9%) | 181.80 (-49.3%) | - | -1.159 |
| | 2.5 | - | 72.25 (+6%) | 178.46 (-50.2%) | - | -1.171 |
| data-driven P-FCUC | 3 | - | 70.21 (+3%) | 241.64 (-32.5%) | - | -1.185 |
| | 2.8 | - | 70.31 (+3.2%) | 241.58 (-32.6%) | - | -1.158 |
| | 2.6 | - | 70.81 (+3.9%) | 202.89 (-43.4%) | - | -1.141 |
| | 2.5 | - | 70.87 (+4%) | 200.08 (-44.2%) | - | -1.151 |
| analytical C-FCUC | - | 0 | 70.11 (+2.9%) | 219.11 (-38.8%) | 0 | -1.650 |
| | - | 20 | 70.12 (+2.9%) | 211.59 (-40.9%) | 0.97 | -1.158 |
| | - | 50 | 70.20 (+3%) | 209.27 (-41.6%) | 2.39 | -1.198 |
| | - | 100 | 70.53 (+3.5%) | 170.1 (-52.5%) | 3.88 | -1.294 |
| data-driven C-FCUC | - | 0 | 69.12 (+1.4%) | 256.93 (-28.3%) | 0 | -1.198 |
| | - | 20 | 69.55 (+2.1%) | 161.05 (-55%) | 0.74 | -1.166 |
| | - | 50 | 69.78 (+2.4%) | 136.44 (-61.9%) | 1.56 | -1.078 |
| | - | 100 | 69.91 (+2.6%) | 130.00 (-63.7%) | 2.97 | -1.147 |

real parameters and thresholds of the current UFLS scheme, and the sum of all possible UFLS in the sample day is calculated. Similarly, the change in percentage compared to the base case is presented. In addition, the cost of real UFLS in the corrective formulations is calculated based on the load-shedding costs associated with each scenario. Finally, the average frequency nadir after all possible outages for each formulation is provided.

To elaborate on the differences between the formulations, a scatter plot of KPIs is presented in Figure 2. The numbers are normalized relative to the BUC to compare the formulations more clearly. For the preventive formulations, the arrow indicates decreasing the nadir threshold, and for corrective formulations, the arrow means increasing UFLS cost.

Comparing different approaches of preventive formulations, it can be seen that the data-driven approach, gives cheaper operation points but would result in higher UFLS costs, indicating that the analytical approach is more conservative. An important assumption in the analytical preventive formulation is that all units would provide their reserve linearly in a constant time T , which is unrealistic and can cause an underestimation of the frequency drop.

The comparison between the two different corrective formulations also gives some insights. In both analytical and data-driven approaches it has been ensured that the net power imbalance is distributed among the available units proportional to their primary frequency control speed. It is observed

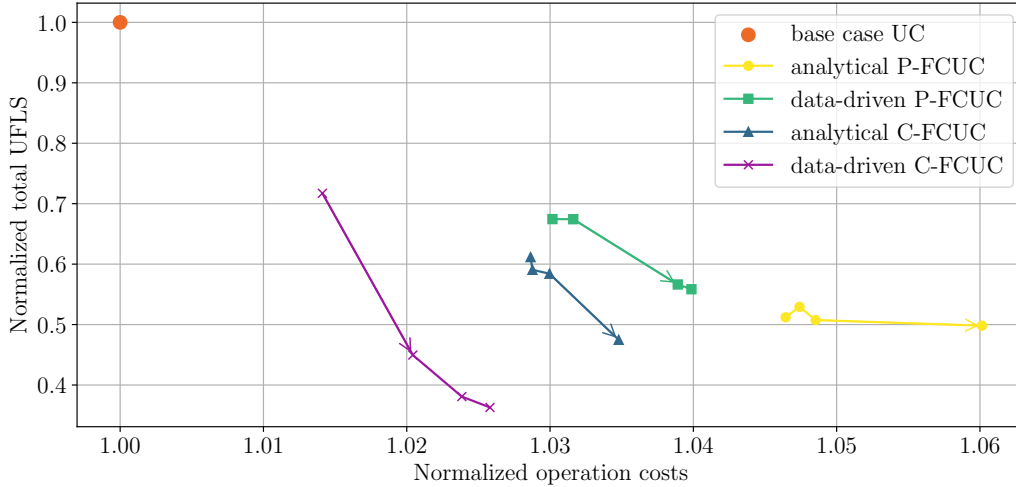


Figure 2: Comparison of system benefits in terms of total UFLS and operation cost

that the data-driven C-FCUC formulation when assigned with UFLS cost, has lower cost and lower total UFLS compared to the analytical C-FCUC. This is mainly because in the analytical C-FCUC formulation it is assumed that the UFLS scheme is adaptive and can be adjusted for each outage. In contrast, traditional UFLS schemes are employed in practice. This will lead to unrealistic estimations of UFLS when compared with the resulting UFLS calculated using the real schemes and parameters of the island power system. In contrast, since the data set used in the data-driven C-FCUC formulation is trained using the real UFLS schemes, it has a more realistic estimation of the UFLS.

Overall, the data-driven C-FCUC formulation, when assigned with UFLS cost, performs better in terms of the system benefits compared to the other formulations. The data-driven C-FCUC has the advantage of having a more realistic estimation of real UFLS which is key to having lower operation cost and overall UFLS in real operation.

The resulting frequency responses of dynamic simulations using SFR model for each formulation with sample thresholds (2.5 Hz for preventive and 50 k€/MW for corrective) and all possible outages are provided in Figure 3. It is observed in Figure 3 that in real operation where conventional UFLS schemes are utilized, all of the formulations can contain frequency after an outage in a relatively timely manner. According to Figure 3, it is important to note that the UFLS scheme used in real operation always man-

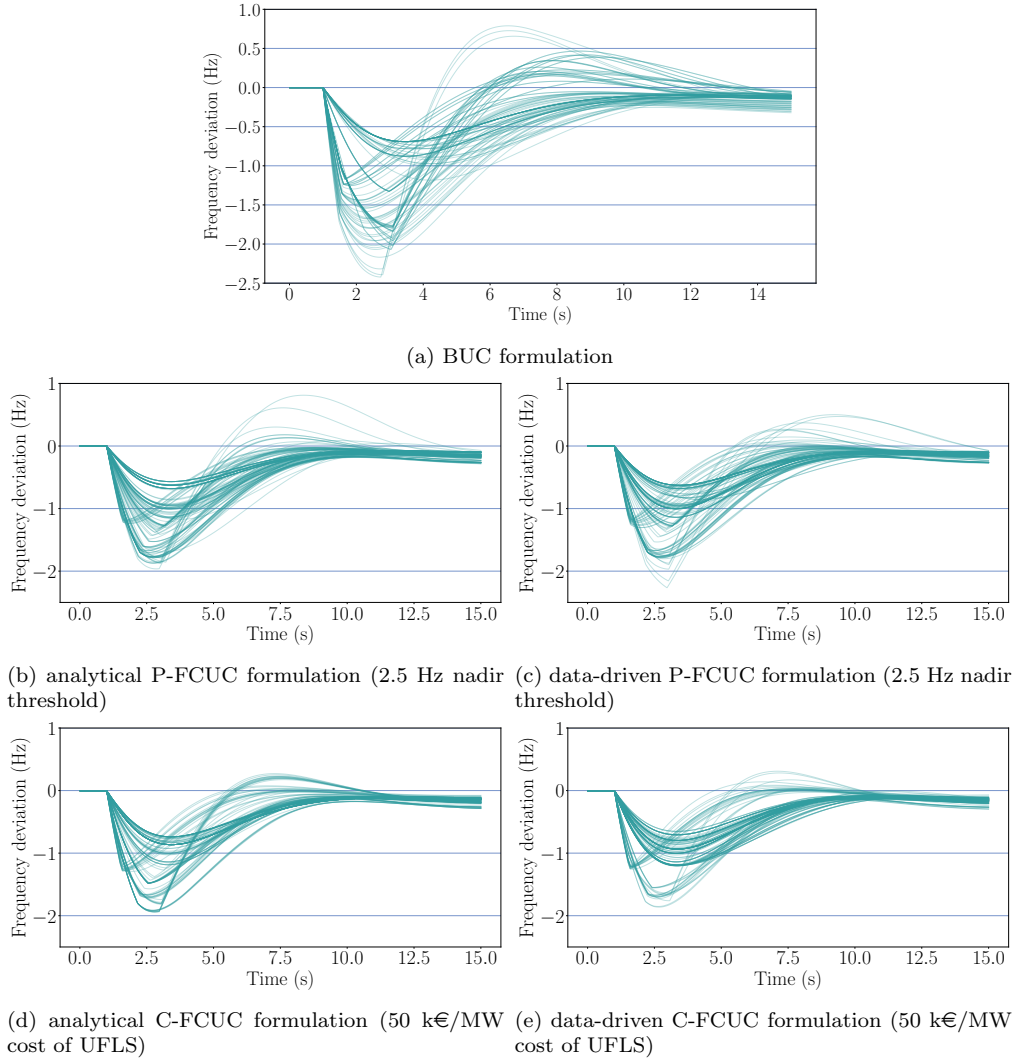


Figure 3: Post-contingency frequency performances

ages to secure the frequency after outages, and no matter what formulation is used the system stability is not jeopardized.

4.3. Computational burden results

Table 4 presents the CPU time, the number of constraints, total variables, and discrete variables for each formulation with different thresholds. It is observed that the corrective formulations generally have higher CPU

Table 4: Computational results

| case study | nadir threshold (Hz) | c^o (k€) | CPU time (s) | constraints | total variables | discrete variables |
|--------------------|----------------------|------------|------------------------|-------------|-----------------|--------------------|
| base case UC | - | - | 7.2 | 6265 | 4513 | 2904 |
| analytical P-FCUC | 3 | - | 167.3 ($\sim 23x$) | 15241 | 14281 | 6864 |
| | 2.8 | - | 123.1 ($\sim 17x$) | 15241 | 14281 | 6864 |
| | 2.6 | - | 113.1 ($\sim 16x$) | 15241 | 14281 | 6864 |
| | 2.5 | - | 104.1 ($\sim 14x$) | 15241 | 14281 | 6864 |
| | 3 | - | 15.5 ($\sim 2x$) | 8113 | 6097 | 2904 |
| data-driven P-FCUC | 2.8 | - | 14.3 ($\sim 2x$) | 8113 | 6097 | 2904 |
| | 2.6 | - | 18.3 ($\sim 2.5x$) | 8113 | 6097 | 2904 |
| | 2.5 | - | 20.1 ($\sim 3x$) | 8113 | 6097 | 2904 |
| analytical C-FCUC | - | 0 | 525.7 ($\sim 73x$) | 24481 | 14281 | 7128 |
| | - | 20 | 518.8 ($\sim 72x$) | 24481 | 14281 | 7128 |
| | - | 50 | 736.1 ($\sim 102x$) | 24481 | 14281 | 7128 |
| | - | 100 | 958.8 ($\sim 133x$) | 24481 | 14281 | 7128 |
| | - | 0 | 146 ($\sim 20x$) | 22105 | 11641 | 3696 |
| data-driven C-FCUC | - | 20 | 633.9 ($\sim 88x$) | 22105 | 11641 | 3696 |
| | - | 50 | 677.1 ($\sim 94x$) | 22105 | 11641 | 3696 |
| | - | 100 | 1497.4 ($\sim 208x$) | 22105 | 11641 | 3696 |
| | - | 100 | 1497.4 ($\sim 208x$) | 22105 | 11641 | 3696 |

times as well as more constraints and variables. The preventive formulations perform better in CPU time and compactness of the problem compared to the corrective formulations.

It can be inferred from Table 4 that the analytical P-FCUC formulation has much higher CPU time compared to the data-driven P-FCUC. However, the data-driven formulation depends on the data set and takes some time offline to train the model. Also, the data set needs to be updated when the system’s structure changes; in that case, the model should be trained again. Changing the nadir threshold in the analytical P-FCUC formulation from 3 to 2.5 Hz, would result in lower CPU times caused by a tighter solution space. Conversely, this change in the data-driven P-FCUC formulation would result in higher CPU times.

According to Table 4, it is noted that the CPU time for the analytical C-FCUC formulation can range from 8 to 16 minutes for the considered case studies. Additionally, the CPU time in this formulation does not necessarily increase when increasing the UFLS cost. In contrast, the data-driven C-FCUC formulation results in CPU times ranging from 2 to 25 minutes, and the solution time increases heavily with increasing the UFLS costs. Similarly, a disadvantage of the data-driven C-FCUC is that it depends on the data set, takes some time offline to train the model, and the data set needs to be updated with every change in the system’s structure.

4.4. Overall performance discussion

The primary aim is to grasp the formulations' operational and computational aspects simultaneously. As discussed previously, in the case of small IPS, the amount of UFLS is the most important metric that distinguishes the performance of each FCUC formulation. Accordingly, two performance indices are introduced. The first index presented in eq. (25) signifies the operational aspect. It is calculated by dividing the increase in operating costs by the total reduction in UFLS compared to the base case. c^{op} represents the operation cost corresponding to the formulation. In other words, this index indicates the additional cost incurred in each formulation to reduce one MW of UFLS.

$$\eta_s = \frac{c^{\text{op}} - c_{\text{BUC}}^{\text{op}}}{\sum p_{\text{BUC}}^{\text{UFLS}} - \sum p^{\text{UFLS}}} \quad (25)$$

The second index reflecting the computational aspect, is presented in eq. (26), where t^{CPU} is the CPU time of the formulation. Similarly, this index is calculated by dividing the amount that the CPU time increases over the BUC, divided by the amount of total UFLS reduction, indicating the amount of time that the solution is prolonged in seconds, to decrease one MW of UFLS.

$$\eta_c = \frac{t^{\text{CPU}} - t_{\text{BUC}}^{\text{CPU}}}{\sum p_{\text{BUC}}^{\text{UFLS}} - \sum p^{\text{UFLS}}} \quad (26)$$

Table 5 gives the numerical results of the performance indices for each formulation. To provide a clearer comparison, Figure 4 illustrates the two proposed indices for all formulations. It is noted that the data-driven C-FCUC formulation shows the best performance regarding the operation cost index, which means that the lowest extra cost should be paid to decrease UFLS, compared to the other formulations.

Alternatively, the data-driven P-FCUC formulation has the best performance regarding the CPU time index showing that it is the fastest among all the formulations. However, it performs poorly in terms of the operation cost index.

Ultimately, choosing the appropriate formulation depends on the operator's preferences in a given situation. This could involve prioritizing a simpler formulation, minimizing the costs associated with UFLS if it is costly, or focusing on reducing operating costs. However, the data-driven C-FCUC formulation appears to have an advantage in most KPIs. It is important to note that the one data-driven C-FCUC point corresponding to a high CPU

Table 5: Performance indices results

| case study | nadir threshold (Hz) | c^o (k€) | cost increase (€) | CPU time increase (s) | UFLS reduction (MW) | η_s | η_c |
|--------------------|----------------------|------------|-------------------|-----------------------|---------------------|----------|----------|
| analytical P-FCUC | 3 | - | 3165 | 160.1 | 174.81 | 18.1 | 0.91 |
| | 2.8 | - | 3231 | 115.9 | 168.62 | 19.2 | 0.69 |
| | 2.6 | - | 3308 | 105.9 | 176.45 | 18.7 | 0.6 |
| | 2.5 | - | 4100 | 96.9 | 179.79 | 22.8 | 0.54 |
| data-driven P-FCUC | 3 | - | 2056 | 8.3 | 116.61 | 17.6 | 0.07 |
| | 2.8 | - | 2155 | 7.1 | 116.67 | 18.5 | 0.06 |
| | 2.6 | - | 2652 | 11.1 | 155.36 | 17.1 | 0.07 |
| | 2.5 | - | 2717 | 12.9 | 158.18 | 17.2 | 0.08 |
| analytical C-FCUC | - | 0 | 1952 | 518.5 | 139.14 | 14 | 3.73 |
| | - | 20 | 1961 | 511.6 | 146.66 | 13.4 | 3.49 |
| | - | 50 | 2042 | 728.9 | 148.98 | 13.7 | 4.89 |
| | - | 100 | 2371 | 951.6 | 188.15 | 12.6 | 5.06 |
| data-driven C-FCUC | - | 0 | 962 | 138.8 | 101.32 | 9.5 | 1.37 |
| | - | 20 | 1392 | 626.7 | 197.2 | 7.1 | 3.18 |
| | - | 50 | 1625 | 669.9 | 221.81 | 7.3 | 3.02 |
| | - | 100 | 1759 | 1490.2 | 228.25 | 7.7 | 6.53 |

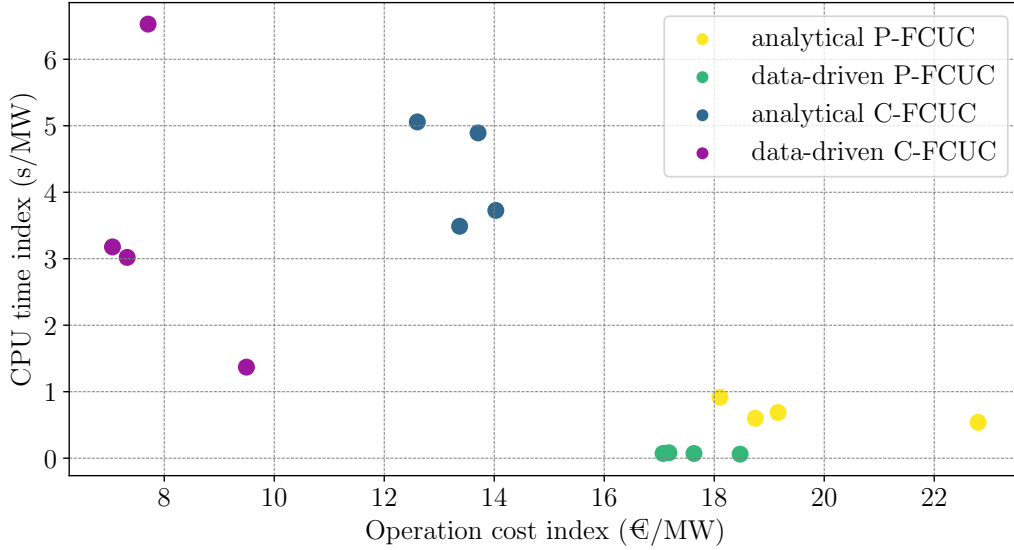


Figure 4: Comparison of the performance indices

time index is the extreme scenario where UFLS cost is considered to be 100 €/MW, which is an extreme cost and unrealistic [19]. It is analyzed here only to evaluate the formulation’s performance thoroughly. The data-driven C-FCUC formulation is competent in the CPU time index with other formulations, excluding the mentioned extreme point. Nevertheless, the data-driven P-FCUC formulation could be utilized when the primary concern is the speed of the formulation.

Table 6: Advantages and disadvantages of the evaluated formulations

| FCUC formulation | Advantages | Disadvantages |
|-------------------------|---|--|
| Analytical P-FCUC | <ul style="list-style-type: none"> - does not require extra offline training time - is faster than corrective formulations - results in lower UFLS than the data-driven P-FCUC | <ul style="list-style-type: none"> - has the highest operation cost index among all the other formulations - some of the assumptions are not realistic. |
| Data-driven P-FCUC | <ul style="list-style-type: none"> - is the fastest among all formulations and has the best CPU time index - is the most compact and adds no binary variable to the BUC formulation | <ul style="list-style-type: none"> - depends on the training data and needs to be updated according to the structure of the system - has an operation cost index higher than the corrective formulations - a different model needs to be trained for each threshold |
| Analytical C-FCUC | <ul style="list-style-type: none"> - has a better operation cost index than the preventive formulations - does not require extra offline training time | <ul style="list-style-type: none"> - has a high CPU time index - gives an unrealistic estimation of the UFLS |
| Data-driven C-FCUC | <ul style="list-style-type: none"> - has the best operation cost index among all formulations - has a more realistic estimation of the UFLS | <ul style="list-style-type: none"> - has a higher CPU time index than the preventive formulations - depends on the training data and needs to be updated according to the structure of the system |

The advantages and disadvantages of each formulation are summarized in Table 6.

5. Conclusions

This paper presents a comparison framework to compare selected formulations of four different FCUC methods with a base case UC formulation. Such a framework enables system operators of IPS to choose an appropriate type of formulation to ensure the frequency stability of the system. Additionally, two performance indices were introduced to analyze each formulation's

system benefits and computational burden, concerning the single most important criteria in IPS which is UFLS. The simulations were conducted on a real Spanish IPS and each formulation's main advantages and disadvantages are presented.

The results show that regarding the system benefits the data-driven C-FCUC formulation leads to the lowest operation cost, most UFLS decrease, and therefore lowest operation cost index. This indicates that the data-driven C-FCUC formulation can be an ideal formulation when the main goals of the operation are the lowest costs and the lowest total resulting UFLS. Moreover, the data-driven P-FCUC shows the best performance regarding the computational burden and the CPU time index indicating that it could be useful when the main goal is to choose the absolute fastest method among others. However, it will lead to a much higher operation cost index than the corrective formulations.

Acknowledgment

This research has been funded by grant PID2022-141765OB-I00 funded by MCIN/AEI/ 10.13039/501100011033 and by “ERDF A way of making Europe”.

References

- [1] L. Sigrist, E. Lobato, F. M. Echavarren, I. Egido, L. Rouco, *Island power systems*, CRC Press, 2016.
- [2] M. Rajabdorri, E. Lobato, L. Sigrist, Robust frequency constrained uc using data driven logistic regression for island power systems, *IET Generation, Transmission & Distribution* 16 (24) (2022) 5069–5083.
- [3] P. Mancarella, F. Billimoria, The fragile grid: The physics and economics of security services in low-carbon power systems, *IEEE Power and Energy Magazine* 19 (2) (2021) 79–88.
- [4] B. Zhou, R. Jiang, S. Shen, Frequency stability-constrained unit commitment: Tight approximation using bernstein polynomials, *IEEE Transactions on Power Systems* (2023).

- [5] M. Tuo, X. Li, Security-constrained unit commitment considering locational frequency stability in low-inertia power grids, *IEEE Transactions on Power Systems* (2022).
- [6] J.-J. Wu, G. W. Chang, C. Sinatra, P.-Y. Tsai, Unit commitment with frequency stability enhancement for an isolated power system, *IEEE Access* (2024).
- [7] Y. Zhang, Q. Guo, Y. Zhou, H. Sun, Frequency-constrained unit commitment for power systems with high renewable energy penetration, *International Journal of Electrical Power & Energy Systems* 153 (2023) 109274.
- [8] C. Ferrandon-Cervantes, B. Kazemtabrizi, M. C. Troffaes, Inclusion of frequency stability constraints in unit commitment using separable programming, *Electric Power Systems Research* 203 (2022) 107669.
- [9] X. Liu, X. Fang, N. Gao, H. Yuan, A. Hoke, H. Wu, J. Tan, Frequency nadir constrained unit commitment for high renewable penetration island power systems, *IEEE Open Access Journal of Power and Energy* (2024).
- [10] L. Liu, Z. Hu, Y. Wen, Y. Ma, Modeling of frequency security constraints and quantification of frequency control reserve capacities for unit commitment, *IEEE Transactions on Power Systems* (2023).
- [11] Y. Zhang, H. Cui, J. Liu, F. Qiu, T. Hong, R. Yao, F. Li, Encoding frequency constraints in preventive unit commitment using deep learning with region-of-interest active sampling, *IEEE Transactions on Power Systems* 37 (3) (2021) 1942–1955.
- [12] L. Sang, Y. Xu, Z. Yi, L. Yang, H. Long, H. Sun, Conservative sparse neural network embedded frequency-constrained unit commitment with distributed energy resources, *IEEE Transactions on Sustainable Energy* 14 (4) (2023) 2351–2363.
- [13] M. Rajabdorri, B. Kazemtabrizi, M. Troffaes, L. Sigrist, E. Lobato, Inclusion of frequency nadir constraint in the unit commitment problem of small power systems using machine learning, *Sustainable Energy, Grids and Networks* 36 (2023) 101161.

- [14] Y. Zuo, G. Frigo, A. Derviškadić, M. Paolone, Impact of synchrophasor estimation algorithms in rocof-based under-frequency load-shedding, *IEEE Transactions on Power Systems* 35 (2) (2020) 1305–1316. doi:10.1109/TPWRS.2019.2936277.
- [15] L. Sigrist, L. Rouco, F. M. Echavarren, A review of the state of the art of ufls schemes for isolated power systems, *International Journal of Electrical Power & Energy Systems* 99 (2018) 525–539. doi:<https://doi.org/10.1016/j.ijepes.2018.01.052>.
URL <https://www.sciencedirect.com/science/article/pii/S0142061517323967>
- [16] F. Ceja-Gomez, S. S. Qadri, F. D. Galiana, Under-frequency load shedding via integer programming, *IEEE Transactions on Power Systems* 27 (3) (2012) 1387–1394.
- [17] R. Bhana, T. J. Overbye, The commitment of interruptible load to ensure adequate system primary frequency response, *IEEE Transactions on Power Systems* 31 (3) (2015) 2055–2063.
- [18] F. Teng, G. Strbac, Full stochastic scheduling for low-carbon electricity systems, *IEEE Transactions on Automation Science and Engineering* 14 (2) (2017) 461–470.
- [19] C. O’Malley, L. Badesa, F. Teng, G. Strbac, Probabilistic scheduling of ufls to secure credible contingencies in low inertia systems, *IEEE Transactions on Power Systems* 37 (4) (2021) 2693–2703.
- [20] M. Rajabdorri, A. Rouco, L. Sigrist, E. Lobato, Unit commitment with analytical under-frequency load-shedding constraints for island power systems, *IEEE Access* (2024).
- [21] M. Rajabdorri, M. C. Troffaes, B. Kazemtabrizi, M. Sarvarizadeh, L. Sigrist, E. Lobato, Data-driven estimation of the amount of under frequency load shedding in small power systems, *Engineering Applications of Artificial Intelligence* 139 (2025) 109617. doi:<https://doi.org/10.1016/j.engappai.2024.109617>.
URL <https://www.sciencedirect.com/science/article/pii/S0952197624017755>

- [22] C. Ferrandon-Cervantes, Secure stochastic unit commitment in low rotational inertia power systems with the inclusion of frequency stability constraints, Ph.D. thesis, Durham University (2021).
- [23] M. Fischetti, J. Jo, Deep neural networks and mixed integer linear optimization, *Constraints* 23 (3) (2018) 296–309.